Solid-State Electronics 53 (2009) 7–10

Contents lists available at ScienceDirect

Solid-State Electronics

journal homepage: www.elsevier.com/locate/sse

4H–SiC ultraviolet avalanche photodetectors with low breakdown voltage and high gain

Huili Zhu [a], Xiaping Chen [a], Jiafa Cai [a], Zhengyun Wu [a,b,*]

[a] Physics Department, Xiamen University, Xiamen 361005, China
[b] MEMS Center, Xiamen University, Xiamen 361005, China

ARTICLE INFO

Article history:
Received 10 June 2007
Received in revised form 2 September 2008
Accepted 12 September 2008
Available online 17 November 2008

The review of this paper was arranged by Prof. Y. Arakawa

PACS:
85.30.−Z
85.30.DE
85.60.Bt
85.60.−q

Keywords:
4H–SiC
Ultraviolet
Avalanche photodetectors (APDs)

ABSTRACT

The separate absorption and multiplication (SAM) 4H–SiC ultraviolet (UV) avalanche photodetectors (APDs) have been designed, fabricated and characterized. A gain higher than 1.8×10^4 was achieved at 90% breakdown voltage of ~55 V. At 0 V, the peak absolute responsivity was estimated to be larger than 0.078 A/W at 270 nm, corresponding to a peak external quantum efficiency of over 35.8%. The long-wavelength cutoff was about 380 nm. In addition, the UV-to-visible rejection ratio of around three orders of magnitude was extracted from the spectra response. When the reverse bias was larger than 35 V, the spectral responsivity enhanced distinctly. At the reverse bias of 42 V, the peak responsivity increased to 0.203 A/W at 270 nm, corresponding to a maximum external quantum efficiency of ~93%, which showed a distinct avalanche behavior. Furthermore, the ideality factor around 1.65 and the spectral detectivity about 3.1×10^{13} cm $Hz^{1/2}$ W^{-1} were estimated. In conclusion, the 4H–SiC APD have excellent performance for UV detection.

1. Introduction

4H–SiC is an attractive material for optical detection in the short-wavelength UV regime owing to its wide bandgap, high thermal conductivity and high critical electric field [1–4]. Photomultiplier tubes (PMTs) are frequently used for these applications because they have high responsivity (600 A/W), high speed and low dark current. However, the PMTs generally require a high-voltage power supply (>1200 V) as well as a cooled photocathode and hence PMT systems are relatively large, expensive, bulky, and fragile. Ultraviolet-enhanced Si APDs can also be used in UV detection systems, but they typically have higher dark currents, i.e., in the nanoampere range at 300 K, require expensive or complex filters for solar-blind operation, and have only demonstrated photon-counting operation down to 400 nm [5]. 4H–SiC APD can exhibit "intrinsically" visible-blind operation and offer a high internal gain by avalanche multiplication, thus improving detection sensitivity. In addition, 4H–SiC material which has a larger ionization coefficient ratio ~10 [6] between holes and electrons is a good candidate for low noise and high gain APDs [2,7,8]. By far, 4H–SiC APDs based on p–n or p–i–n structures have been reported, which can not resolve the trade-off in the maximum achievable photo response, the faster response time and the operating voltage. As SAM-structure has separate high-field multiplication and absorption regions, optimizing the thicknesses and doping concentrations of absorption and multiplication layers, the problem occurred at p–n and p–i–n structure APDs will be resolved. Another benefit of the SAM-APD structure is that only a single type of carrier is injected into the multiplication region, which is a well-known requirement for reducing the multiplication noise that arises from the stochastic nature of the multiplication process [9]. The SAM-APDs have been already deployed in the GaAs based APDs, but unusually in 4H–SiC. The only 4H–SiC SAM-APD had gains of 10^3 near the breakdown voltage >190 V reported by Xiangyi Guo [10]. As for 4H–SiC APDs one design objective is to control the operating voltage to be within 100 V [1]. In this paper, 4H–SiC SAM-APDs with low breakdown voltage (about 55 V) and high photocurrent gain have been fabricated. The electrical and optical properties were characterized.

* Corresponding author. Address: Physics Department, Xiamen University, Xiamen 361005, China. Tel.: +86 592 2180522; fax: +86 592 2189426.
E-mail address: zhywu@xmu.edu.cn (Z. Wu).

0038-1101/$ - see front matter © 2008 Elsevier Ltd. All rights reserved.
doi:10.1016/j.sse.2008.09.002

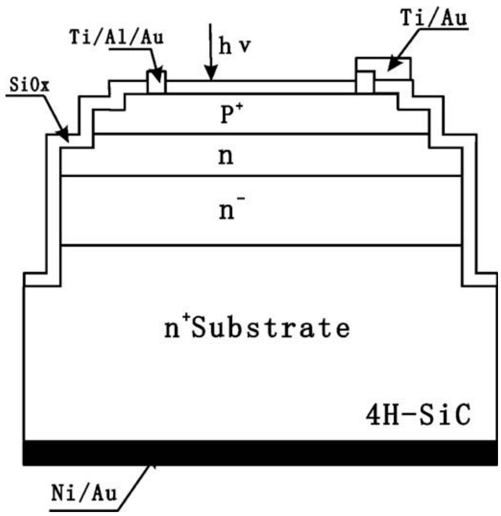

Fig. 1. Schematic cross-section of the 4H–SiC SAM-APD.

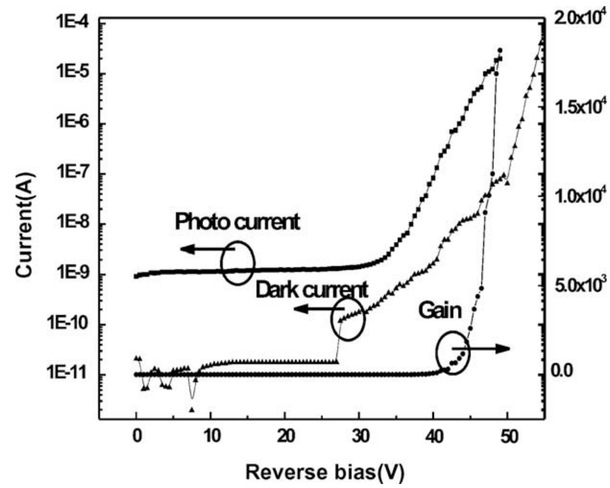

Fig. 2. *I–V* characteristics and gain of 4H–SiC APD.

2. Experiments

Fig. 1 shows the schematic cross-section of the 4H–SiC SAM-APD. The device was fabricated on the n^+ 4H–SiC substrate with three epilayers that consisted of n^-, n and p^+-type layers. In our design, n^+ substrate 4H–SiC APD structure was chosen because of the much higher conductivity of n^+ substrate in comparison to that of p^+ substrate. The top p^+ layer formed the p–n junction together with the n layer, which also served as the multiplication region. The n^- layer acted as both the absorption region and punch-through layer, which absorbed photons and dragged photo-generated holes into the multiplication layer. According to the absorption coefficient of 4H–SiC [10,11], the doping concentrations and thicknesses of n^-, n and p^+ epilayers were designed as 1×10^{15}/cm^3 and 1 μm, <4×10^{17}/cm^3 and 0.25 μm, 5×10^{19}/cm^3 and 0.3 μm, respectively. The multi-step junction extension termination (MJTE) with two 25 μm width steps in the p^+ and n layers were formed by inductively coupled plasmas (ICP) dry etching using a CF_4/O_2 carrier gas mixture. After mesa definition, a thermal oxidation SiO_x passivation layer was applied to the devices. Ti/Al/Au and Ni/Au metals were sputtered on p^+ layer and the backside of n^+ substrate, respectively, and annealed at 900 °C in an Ar ambient to form Ohmic contact. The width of the ring-shaped p-contact metal was 10 μm. Finally, Ti/Au was sputtered as wire-bonding pad. The diameter of optical window was 220 μm. From the linear transmission-line-method (LTLM) patterns, the specific contact resistance and the sheet resistance of p-type contact were determined to be $5.4 \times 10^{-4}\ \Omega\,\mathrm{cm}^2$ and $1.89 \times 10^4\ \Omega/\square$, which showed a good Ohmic behavior.

Photocurrent and dark current were measured using Keithley 2410 source meter and Keithley 6514 system electrometer. The absolute spectral responsivity measurements were performed with a 450 W UV-enhanced Xe arc lamp, an Acton monochrometer with a 2400 g/mm grating, a chopper with a frequency of 2.39 kHz and a lock-in amplifier. The incident power of light illumination on the APDs was calibrated by a UV-enhance Si photodetector from 200 to 400 nm.

3. Results and discussion

Fig. 2 shows the dependence of dark current, photocurrent and the DC gain characteristics with the applied reverse bias of a typical 220 μm-diameter device at room temperature. As can be seen in Fig. 2, the relative low avalanche breakdown voltage about 55 V and significant gain of 1.8×10^4 were achieved. The higher gain occurring at lower biases than typical APD structures [7,10] was due to the SAM-structure. The results showed the 4H–SiC APDs could work at lower reverse voltage with a relatively higher gain, which was very difficult to realize for PMTs. The punch-through voltage was ~27.5 V. Punch-through is the condition at which the edge of the depletion region reaches the absorption layer and photo-generated carriers can be pulled across the barrier at the homointerface. Below punch-through voltage (<27.5 V), the dark current was <10 pA, which was lightly higher than the best result has been reported [12,13]. In addition, the dark current increased with increasing reverse bias. The considered reason was that the mesa sidewall passivation layer could not play a role efficiently. As Xiangyi Guo [4] reported the mesa sidewall leakage current was the major contributor to the device dark current, with the improvement of the sidewall passivation, the dark current of device might be decreased.

The forward current characteristics of the 4H–SiC APD were also analyzed. In theory, APD can be predigested as a p–n junction. According to the thermoionic emission theory, under the low-injection assumption, the forward current can be expressed by Shockley equation:

$$J_F = J_s[\exp(qV/\eta kT) - 1] \tag{1}$$

where η is the ideality factor, k is Boltzmann' constant, q is the electron charge, T is the absolute temperature and J_s is the saturation current. From expressions (1), the ideality factor η and the saturation current J_s can be determined by fitting the linear region of forward current of semi-log *I–V* curve,

$$\eta = \frac{q}{kT}\left[\frac{\partial V}{\partial(\ln J)}\right] \tag{2}$$

Fig. 3 shows the typical forward and reverse *I–V* characteristics of 4H–SiC APD. The forward current of semi-log *I–V* curve showed excellent linearity across seven orders of magnitude. Based on the expressions (2), the ideality factor around 1.65 was obtained, which indicated that the forward current was the cooperation of recombination and diffusion currents. In addition $J_s \sim 5.7 \times 10^{-14}$ A was determined from extrapolation of the intercept to vertical axis in linear fitting of the forward current from the inset of Fig. 3. Note that the leakage current at zero bias was three orders of magnitude higher than the saturation current determined from forward curve. The difference suggested that the saturation current at low bias voltage was unlikely to be the dominating factor and did not present the real leakage current of the SiC photodetector which was similar to the previous report [14].